

Analysis of the Impedance Resonance of Piezoelectric Multi-fiber Composite Stacks

S. Sherrit, A. Djrashian, S C Bradford
Jet Propulsion Laboratory, Caltech, 4800 Oak Grove Dr.
Pasadena, CA, 91109-8099

Abstract – Multi-Fiber Composites™ (MFC's) produced by Smart Materials Corp behave essentially like thin planar stacks where each piezoelectric layer is composed of a multitude of fibers. We investigate the suitability of using previously published inversion techniques [9] for the impedance resonances of monolithic co-fired piezoelectric stacks to the MFC™ to determine the complex material constants from the impedance data. The impedance equations examined in this paper are those based on the derivation by Martin [5,6,10]. The utility of resonance techniques to invert the impedance data to determine the small signal complex material constants are presented for a series of MFC's. The technique was applied to actuators with different geometries and the real coefficients were determined to be similar within changes of the boundary conditions due to change of geometry. The scatter in the imaginary coefficient was found to be larger. The technique was also applied to the same actuator type but manufactured in different batches with some design changes in the non active portion of the actuator and differences in the dielectric and the electromechanical coupling between the two batches were easily measurable. It is interesting to note that strain predicted by small signal impedance analysis is much lower than high field strains. Since the model is based on material properties rather than circuit constants, it could be used for the direct evaluation of specific aging or degradation mechanisms in the actuator as well as batch sorting and adjustment of manufacturing processes.

Keywords: Actuators, Piezoelectric Devices, Multi-fiber composites, Positioners, Resonance Analysis , MFC™

I. INTRODUCTION

Multi-Fiber Composites[1,2,3] have found use in a variety of aerospace, industrial, automatic, and consumer applications where flexible low profile actuation is desired[4]. These MFC's are used in a variety of applications that require relatively high force and larger displacement than single element piezoelectric transducers can produce for a given voltage excitation. These include micro-positioning systems, vibration control, Energy harvesting, shape control, structural health monitoring and ultrasonic transducers. The solution for the zero bond length stack was derived by Martin [5], [6] for the case of piezoelectric. His model was derived from Mason's equivalent circuit of n layers connected mechanically in series and electrically in parallel as shown in Figure 1.

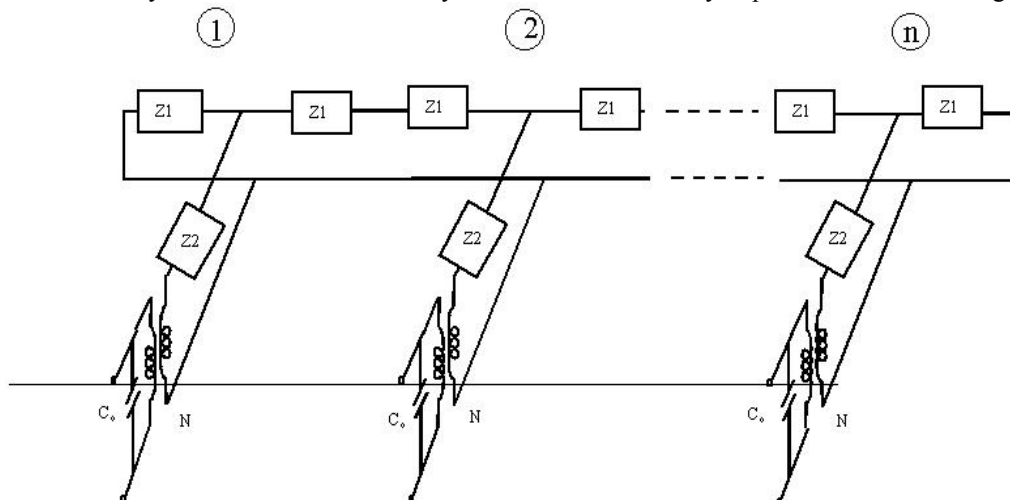


Figure 1. Equivalent circuit representation of a stack with the mechanical ports of each equivalent circuit representing a layer connected in series and n electrical ports in parallel. For stacks with aspect ratios length/width $<$

5 material constants are effective. The MFCTM has a similar structure with each input representing the positive and negative electrodes on the fibers on the MFC and the left and right acoustic ports connect the acoustic ports of the MFC layer to the previous and next layer.

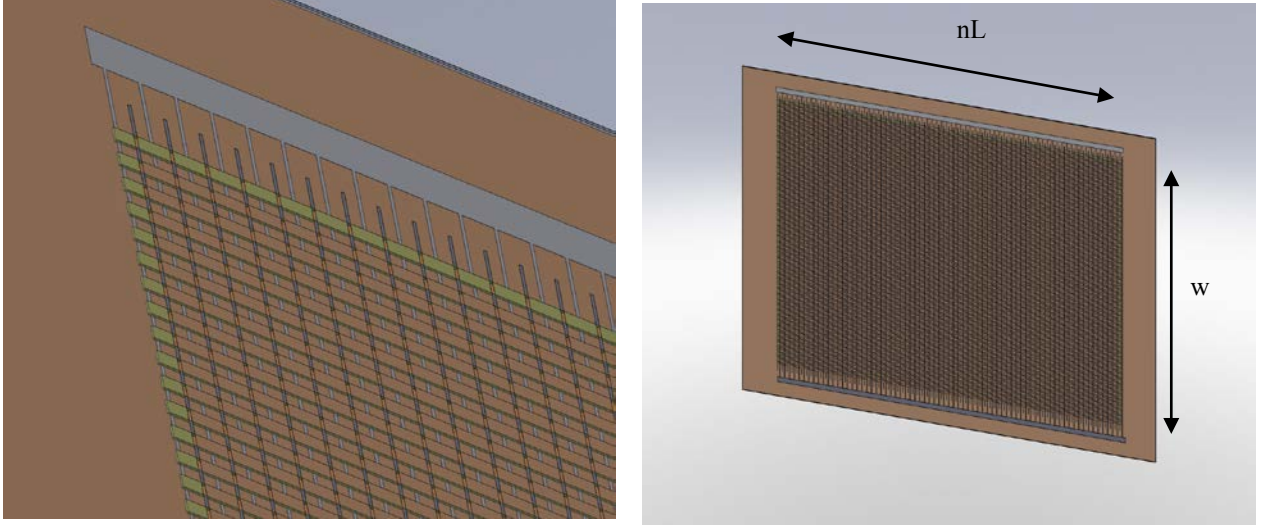


Figure 2. A CAD rendering of an MFC and a close up showing the individual fibers and the positive and negative electrodes.

II. THEORY

The first order equations used to determine the effective elastic, dielectric, and piezoelectric constants in the low frequency limit based on the 3-1 composite theory of Newnham et al.⁷ was published by Wilkie et al.[8] These equations use the volume fraction of the fiber and the matrix material and their elastic constants in the strain direction to calculate the effective material constants of the composite structure. These equations suggest a slight reduction in the piezoelectric properties from the bulk ceramic material however they do not account for dispersion and non linear effects in the ceramic and matrix material.

The overall structure of the MFC's is similar to the structure of a multilayered stack. In the MFC's we have electrodes layers connected in parallel but rather than covering plates of piezoelectric connected mechanically in series they connect a linear array of fibers that are mechanically connected in series to the array of fibers above or below. To a first order approximation the theory for the MFC's should be the same as for Martin's general solution for the admittance of a piezoelectric multilayered stack of plate area A, published earlier [5,6,9,10]. For n layers and total length nL is

$$Y(\omega) = i\omega nC_0 + \frac{2N^2}{Z_{ST}} \tanh\left(\frac{n\gamma}{2}\right) \quad (1)$$

where

$$C_0 = \frac{\epsilon_{33}^T A}{L} (1 - k_{33}^2) \quad (2)$$

$$N = \frac{A d_{33}}{L s_{33}^E} \quad (3)$$

$$Z_{ST} = \left(Z_1 Z_2 \left(2 + \frac{Z_1}{Z_2} \right) \right)^{1/2} \quad (4)$$

$$\gamma = 2 \arcsin h \left(\left(\frac{Z_1}{2Z_2} \right)^{1/2} \right) \quad (5)$$

$$Z_1 = i \rho v^D A \tan \left(\frac{\omega L}{2v^D} \right) \quad (6)$$

$$Z_2 = \frac{\rho v^D A}{i \sin \left(\frac{\omega L}{v^D} \right)} + \frac{iN^2}{\omega C_0} \quad (7)$$

and $v^D = 1/\sqrt{\rho s_{33}^D}$ is the acoustic velocity at constant electric displacement. The constants ϵ_{33}^T , s_{33}^D , d_{33} are the free permittivity, the elastic compliance at constant electric displacement and the piezoelectric charge coefficient, respectively.

In the MFC's the area A is the cross sectional area of the fibers and polymer between the electrodes. In the stack equations above it was assumed that the electrodes are zero thickness but in reality the electrode thickness is non-zero and will change the resonance frequency and the measured elastic constant. In addition the lack of a large aspect ratio (L/w) also can produce changes in the resonance frequency. In the case of the MFC's the electrodes are on the sides of the fibers however due to the large dielectric constant the field lines turn in and produce fields in the piezoelectric that are primarily perpendicular to the electrodes. Due to the lack of the ideal geometry and the fact that the coefficients are for a composite the coefficients determined from the MFC's are to be considered "effective" and this geometry of resonator cannot be used easily to determine the baseline material properties of the piezoelectric material.

Using equations 1 to 7, Martin demonstrated that in the limit of large n (n>8), the acoustic wave speed in the material was determined by the constant field elastic constant s_{33}^E ($v^E = 1/\sqrt{\rho s_{33}^E}$). In the limit of n > 8 an analytical equation for the admittance was presented which allowed for direct determination of material constants from the admittance data [10]. In this limit the admittance was shown to be:

$$\mathbf{Y} = \frac{iAn\omega\epsilon_{33}^T}{L} \left(1 - (\mathbf{k}_{33})^2 + \frac{(\mathbf{k}_{33})^2}{\frac{\omega}{4f_s}} \tan \left(\frac{\omega}{4f_s} \right) \right) \quad (8)$$

where the series resonance frequency is:

$$f_s = \frac{1}{2nL} \sqrt{\frac{1}{\rho s_{33}^E}} \quad (9)$$

In addition to the many layer approximation discussed by Martin, equations 1 to 7 can be shown to reduce to another exact analytical solution in the limit of n = 1 or 2:

$$\mathbf{Z} = \frac{L}{[i\omega n \epsilon_{33}^T (1 - \mathbf{k}_{33}^2) A]} \left[1 - \frac{\mathbf{k}_{33}^2 \tan(\omega/4f_p)}{(\omega/4f_p)} \right] \quad (10)$$

The wave propagates at a speed $v^D = 1/\sqrt{\rho s_{33}^D}$ which is a function of the elastic compliance at constant electric displacement. The parallel frequency constant is:

$$f_p = \frac{1}{2nL} \sqrt{\frac{1}{\rho s_{33}^D}} \quad (11)$$

Equations 8 and 10 can be used to analyze data for stacks with many layers (n>8) and stacks with n = 1 or 2 using Smits' method [11] to determine the effective complex material properties of the piezoelectric material. the limit of large n, the real and imaginary part of the coupling coefficient determined using equation 8 approaches the value determined from the full solution. For n = 1, 2, the results determined using equation 10 are exact although this

solution is typically not of practical interest for MFC's. The standard approach (which is valid for all values of n) is to directly fit equation 1 to the data using non-linear regression techniques for complex parameters as has been done for bulk [12] and thin film [13] and stack resonators[9]. The material constants shown in equation 8 are effective constants. To determine the material properties one has to account for the segmentation and divide the d_{33} coefficient by n to get the material d_{33} . Also the dielectric constant of the material is found by dividing the effective dielectric constant by n^2 .

An alternative to the full non linear regression to determine the complex coefficients one can use the admittance equation shown in equation 8 and Smits method to evaluate the effective complex material constants. A mapping of the critical frequencies in equation 8 to the Butterworth Van Dyke Circuit model allows the use of the IEEE standard method [14] to determine the relationships between the resonance frequency f_s and the elastic constant and the coupling from the resonance and anti-resonance frequency. The effective real parts of the constants and the mechanical Q of a many layer approximation in equation 8 can be determined by matching the best fit to the Butterworth Van Dyke circuit constants as is shown in Table 1.

Table 1. Stack effective parameters determined from Butterworth Van Dyke Circuit (C_0, C_1, L_1, R_1). (L =stack length, A=effective cross sectional area , ρ = effective density)

Resonance frequency f_s Anti-resonance frequency f_p	$f_s = \frac{1}{2\pi\sqrt{L_1 C_1}} \approx f_r$ $f_p = \frac{1}{2\pi\sqrt{L_1 \frac{C_0 C_1}{C_0 + C_1}}}$
Circuit Q \approx Mechanical Q	$Q = \frac{1}{R_1} \sqrt{\frac{L_1}{C_1}}$
Coupling coefficient	$\frac{k_{33}^2}{1 - k_{33}^2} = \frac{\pi f_p}{2 f_s} \tan\left(\frac{\pi f_p - f_s}{2 f_s}\right)$
Effective elastic constant (m^2/N)	$s^E = \frac{1}{4\rho f_s^2 L^2}$
Effective dielectric permittivity (F/m)	$\epsilon_{LF} = \frac{L}{A}(C_1 + C_0)$
Effective piezoelectric constant = Stroke/volt (m/V)	$d_{33}^{eff} = \sqrt{k_{33}^2 s^E \epsilon_{LF}}$

III. RESULTS

The actuators measured in this study are shown in Figure 3. In order to look at the sensitivity of these resonance methods we have evaluated the MFC#1 (M8528-P1 – 02F10-0321) using Smits resonance analysis [11] about the fundamental and the 5th resonance peak. The data determined from each of these analyses are shown in Table 2 and 3. The data and the fit to the data are shown in Figure 4 and 5. From the data it is clear that there is substantial dispersion in the material coefficients with the resonator becoming stiffer and mechanically less lossy (Q) at higher frequencies. The piezoelectric response and dielectric constant are also reduced as the frequency is increased. This dispersion could be the result of the elastic properties of the matrix material stiffening as the frequency increases, behaving more like a glass than a polymer. In addition it is clear from the data that the

fundamental resonance has sideband resonance nearby due to lateral modes which can distort the analysis. The strain from the resonance measurements at the fundamental resonance extrapolated to high fields for the MFC's is about 10 times less than the measured high field strain. The reduction is even more significant for the data determined from the 5th resonance mode. Typically the small signal piezoelectric coefficient is about a factor of 2 or more smaller than the large signal piezoelectric coefficient in bulk ceramics due to domain effects[15]. From the data in Table 2 and 3 we can see a reduction in the small signal piezoelectric response is about 50 percent between 20 kHz and 200 kHz. This level of dispersion is generally not seen in bulk ceramic stacks at these frequency ranges. This suggests that much of the additional decrease in the small signal strain is due to dispersion in the material properties.

We have looked at two nominal MFC's with the same overall active dimensions but produced in different batches at different times and after modifications were made to the process. The earlier 17C10 batch had a longer and wider overall footprint even though the active area was similar. To determine if the technique is sensitive enough to determine the effects of minor process changes. The analysis results for the MFC#2 (M8528-P1 - 17C10-0261) are shown in Tables 4 and 5 for the fundamental and 5th resonance mode. The data and the fit to the 5th resonance is shown in Figure 6.

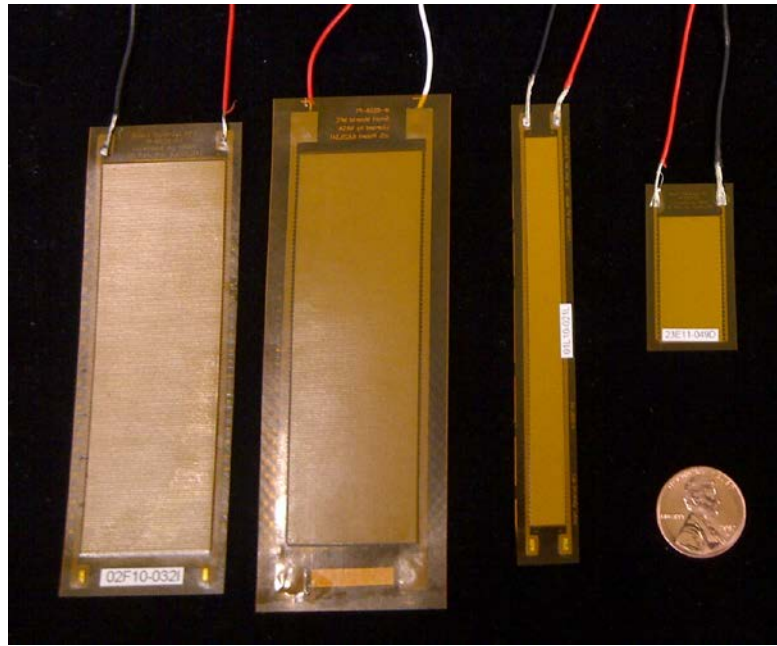


Figure 3. The four MFC actuators measured in this study. The two MFC's on the left are nominally the same dimensions but from a different batch and after processing changes.

Table 2: The effective material properties for the data of the MFC- 02F10 stack resonator shown in Figure 4. The stack length $nL = 0.0875\text{m}$, Area $A = 0.00000825\text{ m}^2$ and density $\rho = 5400\text{ kg/m}^3$. The fit was evaluated around the fundamental resonance.

Property	Real	Imaginary
s_{33}^E (m^2/N)	1.85×10^{-11}	-8.3×10^{-13}
ϵ_{33}^T (F/m)	1.89×10^{-9}	-3.7×10^{-11}
d_{33} (C/N)	61.0×10^{-12}	-2.42×10^{-12}
k_{33}	0.334	-0.0012

Table 3: The effective material properties for the data of the MFC –2F10 stack resonator shown in Figure 5. The stack length $nL = 0.0875\text{m}$, Area $A = 0.00000825\text{ m}^2$ and density $\rho = 5400\text{ kg/m}^3$. The fit was evaluated around the 5th resonance.

Property	Real	Imaginary
s_{33}^E (m ² /N)	1.49×10^{-11}	-2.4×10^{-13}
ϵ_{33}^T (F/m)	1.68×10^{-9}	-4.1×10^{-11}
d_{33} (C/N)	40×10^{-12}	-1.5×10^{-12}
k_{33}	0.252	-0.0047

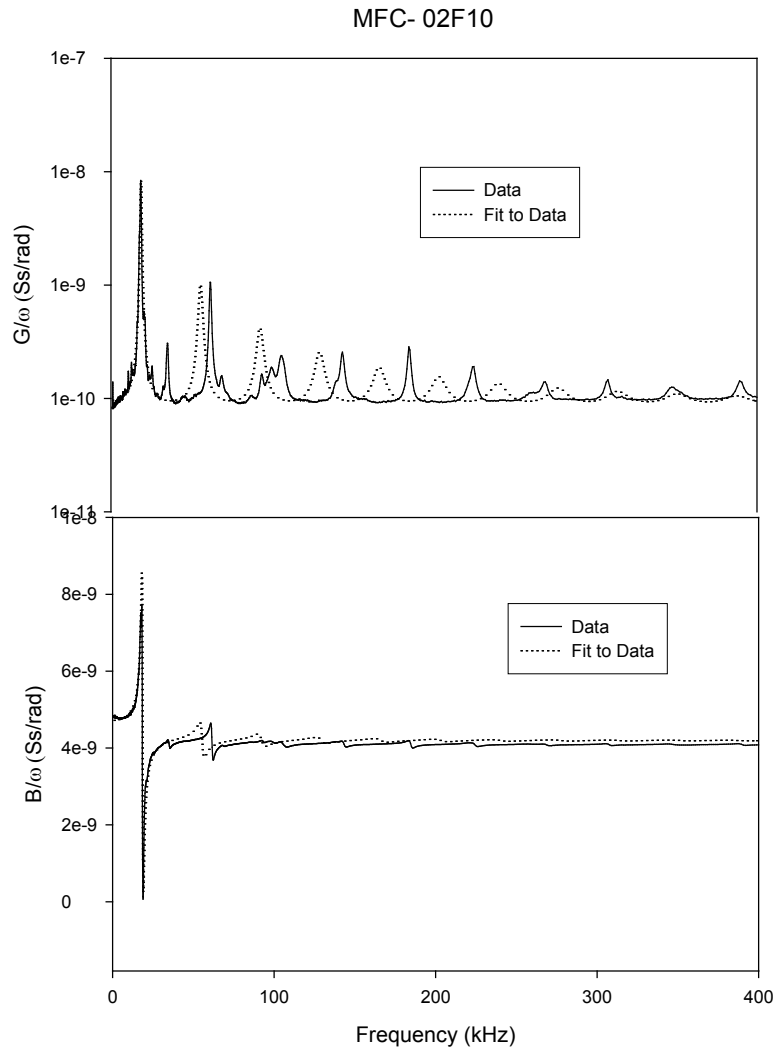


Figure 4. The conductance and susceptance divided by angular frequency for an 8.5 cm, 2.75 cm wide and 0.3 mm thick MFC (02F10) as a function of frequency for $n=170$ layers. The solid line is the data and the dashed line is the fit to the fundamental resonance using equation 8. The data from the fit is in Table 2.

The resonance data in Figure 6 is roughly similar to the data in Figure 4 and 5 however there are measurable differences in material constants determined from the fit to the data. The fundamental resonance is weaker and noisier than the fundamental resonance in the MFC – 02F10 resonator. In addition the baseline of the G/ω curve which is related to $\tan\delta$ is seen to have a significant slope. The piezoelectric response of the earlier batch 17C10 was found to be smaller and the coupling measured at the fundamental resonance was significantly reduced. The properties at the 5th resonance at about 200 kHz seem to align. It is possible that the extra material on the ends and widths enhanced the coupling to the width resonance and obscured the fundamental resonance and reduce the coupling.

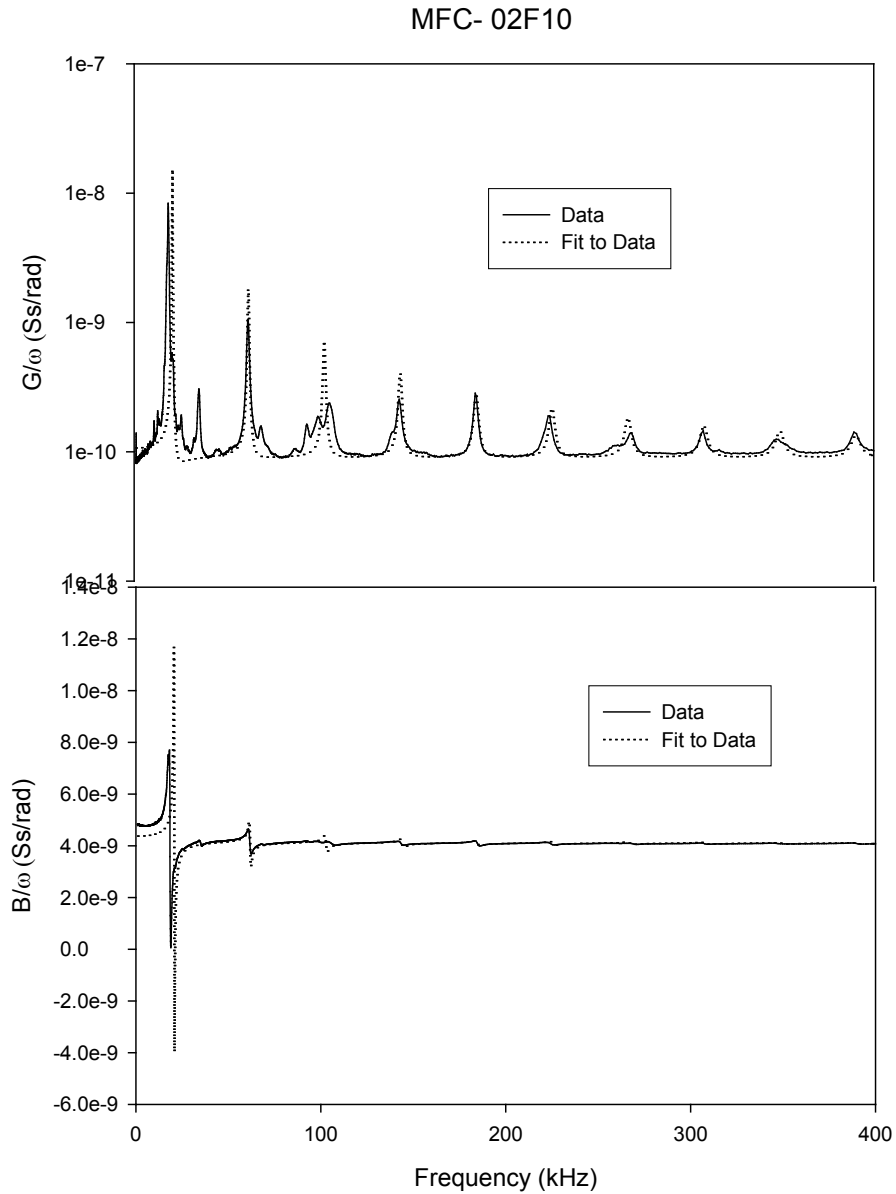


Figure 5. The conductance and susceptance divided by angular frequency for an 8.5 cm, 2.75 cm wide and 0.3 mm thick MFC (MFC-02F10) as a function of frequency for $n=170$ layers. The solid line is the data and the dashed line is the fit using equation 8 about the 5th resonance and the material data determined from the fit is in Table 3.

Table 4: The effective material properties for the data of the MFC- 17C10 stack resonator shown in Figure 6. The stack length $nL = 0.0875\text{m}$, Area $A = 0.00000825\text{ m}^2$ and density $\rho = 5400\text{ kg/m}^3$. The fit was evaluated around the fundamental resonance.

Property	Real	Imaginary
s_{33}^E (m^2/N)	1.79×10^{-11}	-1.13×10^{-12}
ϵ_{33}^T (F/m)	1.44×10^{-9}	-3.7×10^{-11}
d_{33} (C/N)	$36. \times 10^{-12}$	-6.5×10^{-12}
k_{33}	0.226	-0.031

In general the results between the two batches at high frequencies are similar for each of the 17C10 and 02F10 batches. The major differences are found at the fundamental resonance. We chose the 5th resonance to evaluate since it is the first resonance that shows no distortion from sidebands.

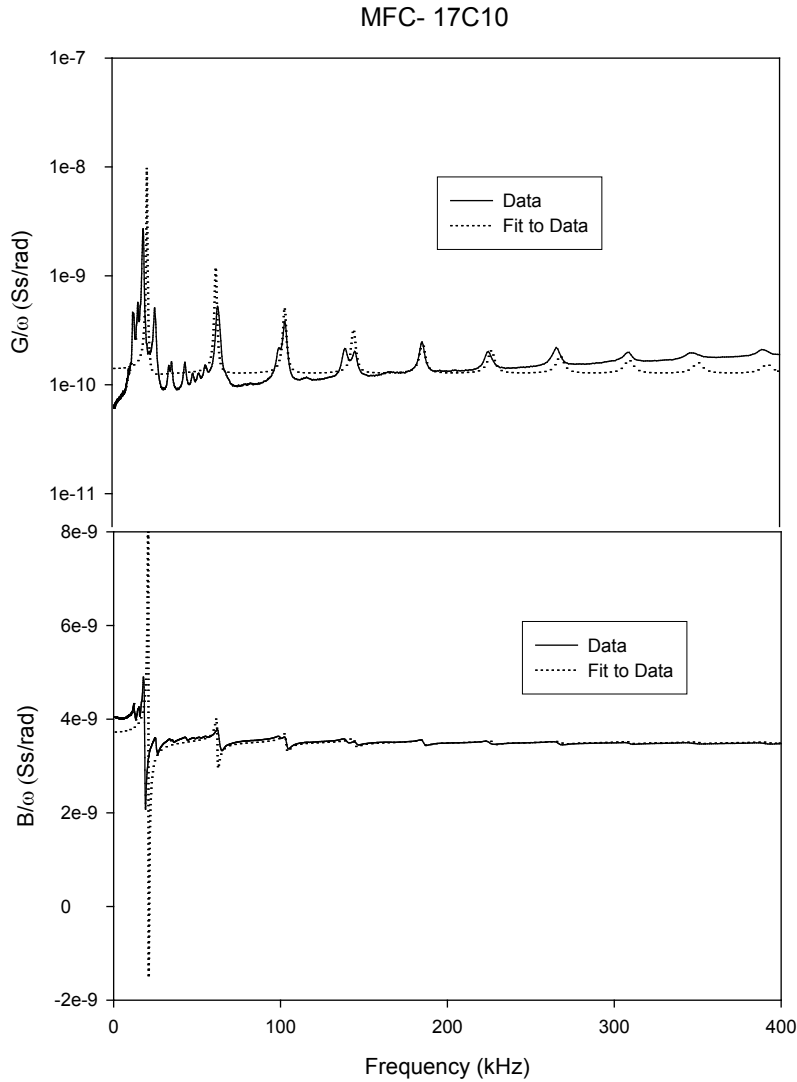


Figure 6. The conductance and susceptance divided by angular frequency for an 8.5 cm, 2.75 cm wide and 0.3 mm thick MFC (MFC-17C10) as a function of frequency for $n=170$ layers. The solid line is the data and the dashed line is the fit using equation 8 about the 5th resonance and the material data determined from the fit is in Table 5.

Table 5: The effective material properties for the data of the MFC- 17C10 stack resonator shown in Figure 6. The stack length $nL = 0.0875\text{m}$, Area $A = 0.00000825\text{ m}^2$ and density $\rho = 5400\text{ kg/m}^3$. The fit was evaluated around the 5th resonance.

Property	Real	Imaginary
s_{33}^E (m ² /N)	1.48×10^{-11}	-2.7×10^{-13}
ϵ_{33}^T (F/m)	1.34×10^{-9}	-5.1×10^{-11}
d_{33} (C/N)	35×10^{-12}	-1.4×10^{-12}
k_{33}	0.245	-0.0032

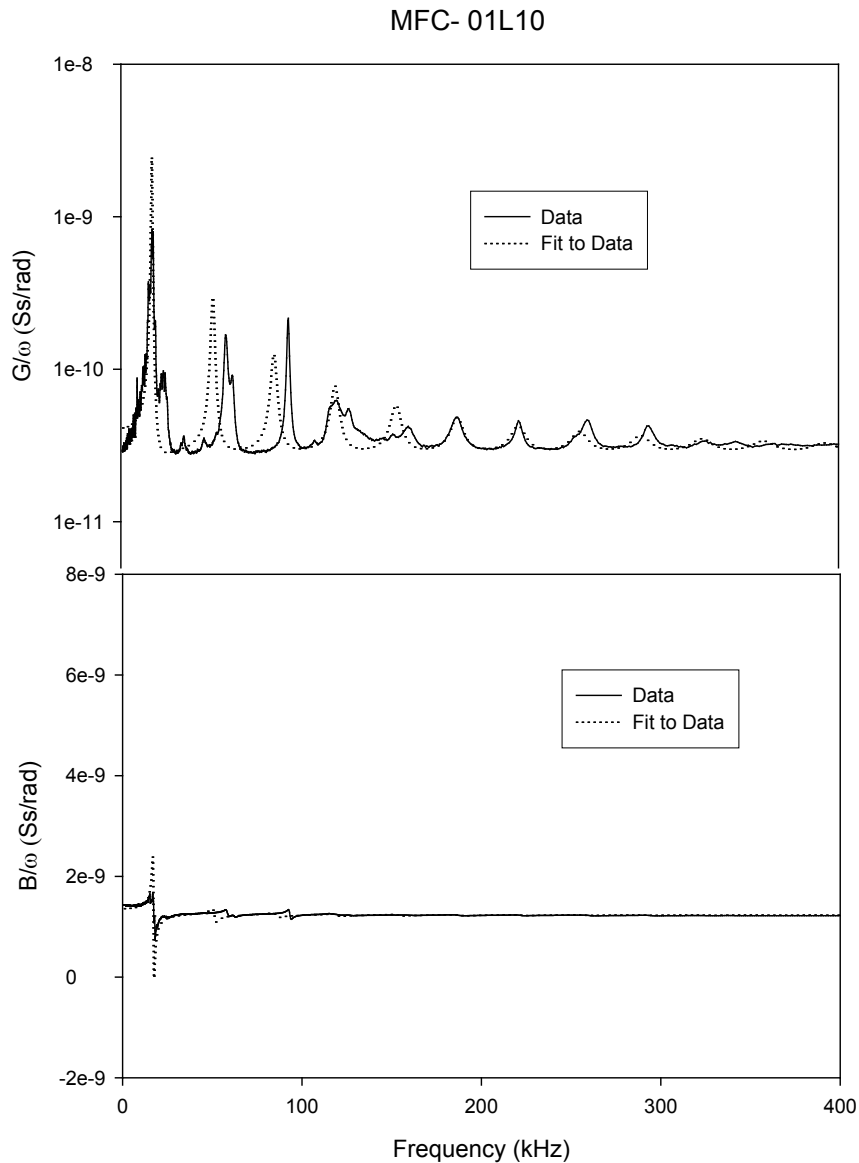


Figure 7. The conductance and susceptance divided by angular frequency for an 8.5 cm, 0.75 cm wide and 0.3 mm thick MFC (MFC-01L10) as a function of frequency for $n=170$ layers. The solid line is the data and the dashed line is the fit using equation 8 about the 6th resonance and the material data determined from the fit is shown in Table 6.

Table 6: The effective material properties for the data of the MFC –01L10 stack resonator shown in Figure 7. The stack length $nL = 0.0875\text{m}$, Area $A = 0.00000225\text{ m}^2$ and density $\rho = 5400\text{ kg/m}^3$. The fit was evaluated around the 6th resonance.

Property	Real	Imaginary
s_{33}^E (m ² /N)	2.17×10^{-11}	-9.5×10^{-13}
ϵ_{33}^T (F/m)	1.764×10^{-9}	-5.3×10^{-11}
d_{33} (C/N)	61×10^{-12}	-4.5×10^{-12}
k_{33}	0.311	-0.011

The results of the analysis of the long thin MFC (01L10) and the short MFC (23E11) are shown in Figures 7 and 8 and in Table 6 and 7. The data for the long thinner MFC was determined by a fit to the first clean resonance (6th) while the material coefficients were determined from the fundamental resonance in the short MFC. The shorter MFC had a larger effective dielectric constant and a lower mechanical Q while the coupling was found to be comparable in both MFCs.

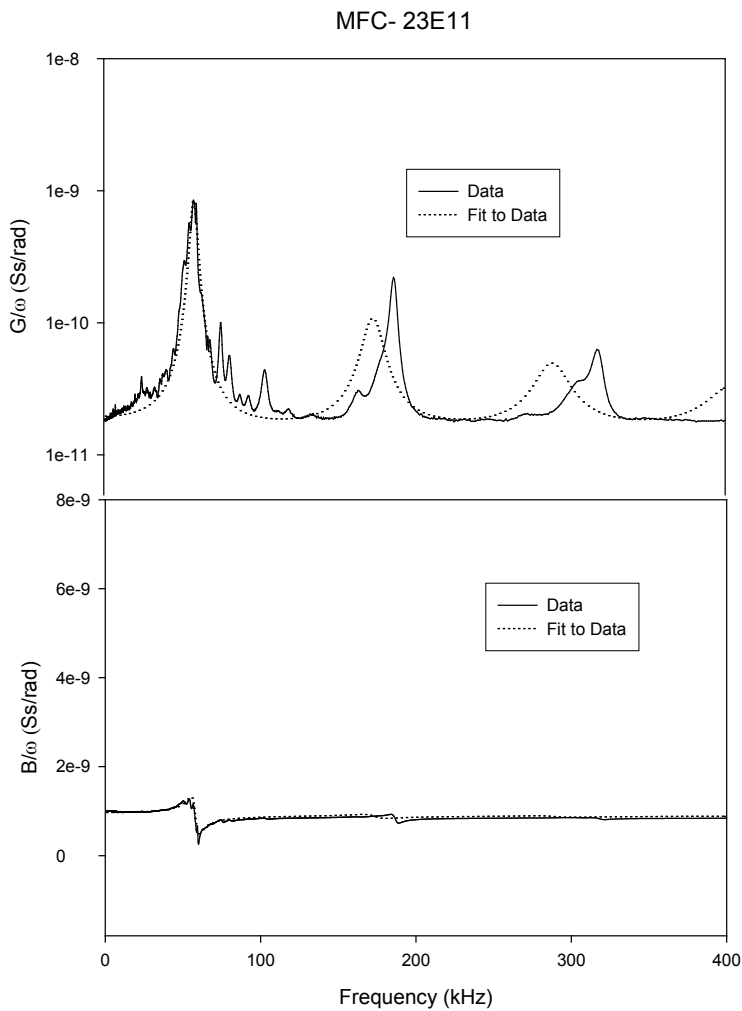


Figure 8. The conductance and susceptance divided by angular frequency for an 2.6 cm long, 1.35 cm wide and 0.3 mm thick MFC (MFC-23E11) as a function of frequency for $n=50$ layers. The solid line is the data and the dashed line is the fit using equation 8 about the 1st resonance and the material data determined from the fit is shown in Table 7.

Table 7: The effective material properties for the data of the MFC –23E11 stack resonator shown in Figure 8. The stack length $nL = 0.026\text{m}$, Area $A = 0.00000405\text{ m}^2$ and density $\rho = 5400\text{ kg/m}^3$. The fit was evaluated around the fundamental resonance.

Property	Real	Imaginary
s_{33}^E (m^2/N)	2.09×10^{-11}	-1.82×10^{-12}
ϵ_{33}^T (F/m)	2.48×10^{-9}	-5.0×10^{-11}
d_{33} (C/N)	69×10^{-12}	-4.8×10^{-12}
k_{33}	0.303	-0.005

In addition the compliance of the short and thin MFC's were found to be larger than the MFC's measure in Tables 2-5. This could be due to the increased fraction of polymer material to piezoelectric material in the MFC in these configurations. The resonance analysis above demonstrated that dispersion in the material properties is a major factor for the inability of the small signal resonance data to predict the large signal response. This initial study of the resonator geometries suggest that material properties determined from the resonators were remarkably similar (excluding the earlier MFC 17C10) given the large change in geometry and that they could be used to distinguish process changes during manufacturing.

It would be interesting to look at the dispersion in these resonators in more depth since this is critical to the predictive ability in the low frequency performance from the small signal resonance analysis. Future studies which we believe may help in sorting out the source of the dispersion include;

1. Inter-batch studies of identical resonators to determine the standard errors of the method,
2. High field, high frequency studies of resonators under duty cycle(remove thermal effects) to determine nonlinear effects,
3. Build sets of resonators and adjust only the length and keep the width constant and measure the properties and see how the change in length changes the effective material properties. Alternatively only adjust the width.
4. Resonance studies while bonded on substrates. The network models could be used to account for the substrate stiffness and shifts in frequencies.

IV. CONCLUSIONS

A model for the impedance resonance of a MFC stack resonator was presented based on the similarities to the multilayer stack structure which allowed for non-destructive evaluation of the material properties of the Multi-fiber composite. The model was shown to reduce to standard resonance equations in the limit of many electrode layers. In the case where only real coefficients were required a table was presented showing the relationship of the Butterworth Van-Dyke Circuit constants and the material coefficients. A set of multi-layer stack resonators were tested and the impedance spectra fit using Smits method on the many layer approximation model shown in equation 8. Sizeable dispersion in the material coefficients including the electromechanical coupling was measured. The constants determined from fitting the data to higher order resonances were found to be in general agreement with each other. The small signal material coefficients predicted strain levels that were a factor of 10 less than strain levels measured using the low frequency data. The discrepancy was suggested to be due to both non-linearities and dispersion in the effective material constants of the resonator. It is suggested that future studies look at methods to determine the source of the dispersion.

ACKNOWLEDGMENT

The research at the Jet Propulsion Laboratory (JPL), a division of the California Institute of Technology, was carried out under a contract with the National Aeronautics Space Agency (NASA). Reference herein to any specific

commercial product, process, or service by trade name, trademark, manufacturer, or otherwise, does not constitute or imply its endorsement by the United States Government or the Jet Propulsion Laboratory, California Institute of Technology.

REFERENCES

- [1] A.A. Bent, "Active Fiber Composite Material Systems for Structural Control Applications," In: Proceedings, SPIE's 6th International Symposium on Smart Structures and Materials, vol 3674, March 1–5, Newport Beach, CA., 1999
- [2] A.A. Bent, and N.W. Hagood, "Piezoelectric Fiber Composites with Interdigitated Electrodes," Journal of Intelligent Material Systems and Structures, November 1997.
- [3] W.K. Wilkie, R. G. Bryant, J. W. High, R.L. Fox, R.F. Hellbaum, A. Jalink, Jr., B.D. Little, and P.H. Mirick, "Low-Cost Piezocomposite Actuator for Structural Control Applications," Proceedings SPIE's 7th International Symposium on Smart Structures and Materials, vol. 3991, March 5–9, Newport Beach, California, 2000.
- [4] Smart Material Corporation webpage - <http://www.smart-material.com/MFC-product-main.html> [downloaded Dec 2022]
- [5] G.E. Martin, "Vibrations of Coaxially Segmented Longitudinally Polarized Ferroelectric Tubes", JASA 36, pp. 1496-1506, August 1964.
- [6] G.E. Martin, "On the Theory of Segmented Electromechanical Systems" JASA, 36, pp 1366-1370.
- [7] R.E. Newnham, D. Skinner, and L. Cross, "Connectivity and Piezoelectric-Pyroelectric Composites", Materials Research Bulletin, 13:525–536. 1978
- [8] W. Keats Wilkie, Daniel J. Inman, Justin M. Lloyd and James W. High, "Anisotropic Laminar Piezocomposite Actuator Incorporating Machined PMN–PT Single-Crystal Fibers", Journal Of Intelligent Material Systems And Structures, Vol. 17, pp. 15- 28, January 2006
- [9] S. Sherrit, S.P. Leary, B.P. Dolgin, Y. Bar-Cohen, R. Tasker, "The Impedance Resonance for Piezoelectric Stacks", Proceedings of the IEEE Ultrasonics Symposium, pp. 1037- 1040, San Juan, Puerto Rico, Oct 22-25, 2000
- [10] G.E. Martin, "New Standard for Measurements of Certain Piezoelectric Ceramics" JASA, 35, pp.925(L), 1963
- [11] J.G. Smits, "Iterative Method for Accurate Determination of the Real and Imaginary Parts of Materials Coefficients of Piezoelectric Ceramics, IEEE Trans on Sonics and Ultrasonics, (SU-23),(6), pp. 393-402, November, 1976.
- [12] K.W. Kwok, H.L. Chan, C.L. Choy, " Evaluation of the Material Parameters of Piezoelectric Materials by Various Methods", IEEE Trans. on Ultrasonics, Ferroelectrics and Frequency Control, 44, (4), pp. 733-742, July 1997
- [13] M. Lukacs, T. Olding, M. Sayer, R. Tasker, and S. Sherrit, " Thickness mode material constants of a supported piezoelectric film", J. Appl. Phys. 85, pp. 2835-2843, March 1999
- [14] IEEE/ANSI Std 176-1987, IEEE Standard on Piezoelectricity
- [15] S. Sherrit, H.D. Wiederick, B.K. Mukherjee, "The Field Dependence of the Complex Piezoelectric, Dielectric, and Elastic Properties of Motorola PZT 3203 HD Ceramic" SPIE Proceedings of the International Society for Optical Engineering Symposium on Smart Structures and Materials, March, Vol 3040, pp 99-109, March 1997